Role of Histogram Features on Arterial Spin Labeling Perfusion Magnetic Resonance Imaging in Identifying Isocitrate Dehydrogenase Genotypes and Glioma Malignancies

Changliang SU[1], Chuan PENG[1], Yifan SUN[2], Frederick C. DAMEN[3], Rifeng JIANG[2], Chuanmiao XIE[1], Kejia CAI[3]

[1]Department of Medical Imaging, State Key Laboratory of Oncology in South China, Guangdong Provincial Clinical Research Center for Cancer, Sun Yat-Sen University Cancer Center, Guangzhou 510060, P. R. China
[2]Fujian Medical University Union Hospital, Department of Radiology, Fuzhou, 350001, China
[3]University of Illinois at Chicago, College of Medicine, Department of Radiology, Chicago, IL, USA

Corresponding author: Chuanmiao XIE ✉ xchuanm@sysucc.org.cn

ABSTRACT

AIM: To explore the use of histogram features on noninvasive arterial spin labeling (ASL) perfusion magnetic resonance imaging (MRI) in differentiating isocitrate dehydrogenase mutant-type (IDH-mut) from isocitrate dehydrogenase wild-type (IDH-wt) gliomas, and lower-grade gliomas (LGGs) from glioblastomas.

MATERIAL and METHODS: This retrospective study included 131 patients who underwent ASL MRI and anatomic MRI. Cerebral blood flow (CBF) maps were calculated, from which 10 histogram features describing the CBF distribution were extracted within the tumor region. Correlation analysis was performed to determine the correlations between histogram features as well as tumor grades and IDH genotypes. The independent t-test and Fisher's exact test were used to determine differences in the extracted histogram features, age at diagnosis, and sex in different glioma subtypes. Multivariate binary logistic regression analysis was performed, and diagnostic performances were evaluated with the receiver operating characteristic curves.

RESULTS: CBF histogram features were significantly correlated with tumor grades and IDH genotypes. These features can effectively differentiate LGGs from glioblastomas, and IDH-mut from IDH-wt gliomas. The area under the receiving operating characteristic curve of the model calculated using combined CBF 30th percentile and age at diagnosis in differentiating LGGs from glioblastomas was 0.73. Integrating age at diagnosis and CBF 10th percentile could be more effective in differentiating IDH-mut from IDH-wt gliomas. Furthermore, the combined model had a better area under the receiving operating characteristic curve at 0.856 (sensitivity: 84.4%, specificity: 82.9%).

CONCLUSION: The histogram features on ASL were significantly correlated with tumor grade and IDH genotypes. Moreover, the use of these features could effectively differentiate glioma subtypes. The combined application of age at diagnosis and perfusion histogram features resulted in a more comprehensive identification of tumor subtypes. Therefore, ASL can be a noninvasive tool for the pre-surgical evaluation of gliomas.

KEYWORDS: Gliomas, Isocitrate Dehydrogenase, Arterial spin labeling, perfusion MRI, Histogram, Radiology, Diagnosis

Changliang SU 🆔 : 0000-0002-4418-5823
Chuan PENG 🆔 : 0000-0002-3258-5774
Yifan SUN 🆔 : 0000-0001-8900-0119
Frederick C. DAMEN 🆔 : 0000-0002-3049-3083
Rifeng JIANG 🆔 : 0000-0001-6959-0027
Chuanmiao XIE 🆔 : 0000-0002-9211-8609
Kejia CAI 🆔 : 0000-0003-1511-4273

■ INTRODUCTION

Gliomas are the most common primary brain tumors that cause severe neurone dysfunction and irreversible damage to patient health (25). Gliomas are generally divided into four grades (I, II, III, and IV). Among them, grade IV glioblastoma is the most aggressive type, with a 5-year overall survival rate of <5% (22,35). In contrast, grade II and III gliomas have a median survival of >7 years and are collectively referred to as diffuse lower-grade gliomas (LGGs) (2). Due to their different molecular features, gliomas with identical tumor grades respond differently to therapeutic schedules. Moreover, they have different therapeutic outcomes (33,34). Integrating phenotypic and genotypic information for glioma management in clinical settings can reduce relapse rate and prolong patient survival (22). Isocitrate dehydrogenase (IDH) is an important genetic biomarker driving glioma genesis that can distinguish biological features in different glioma subtypes (1). IDH mutant-type (IDH-mut) gliomas are more responsive to surgical resection and have a better survival outcome from maximal surgical resection than IDH wild-type (IDH-wt) gliomas (14). Mutant IDH status is an indicator of enhanced chemosensitivity (31), and is associated with a better post-surgical quality of life in patients with high-grade glioma (20). Histopathologic examinations using tumor tissue samples obtained via craniotomy or biopsy are the gold standards for glioma diagnosis. However, the application of such tests may be inhibited by several issues. First, the potential risks and complications of craniotomy can affect patient health. Second, the diagnosis and treatment of patients with glioma might become an issue in failed genetic detection or pathologic examination caused by unsatisfactory tissue sampling or unsuccessful testing. The noninvasive identification of IDH types and glioma malignancies on functional magnetic resonance imaging (MRI), which is an alternative method, can provide important references for clinical diagnosis. Additionally, the noninvasive identification of IDH types and glioma malignancies can facilitate treatment planning, and has a possible effect on the patient's willingness to accept proposed treatments. Noninvasive methods can significantly affect clinical practices in monitoring treatment effects and identifying glioma recurrence. IDH-mut gliomas generate a distinct metabolic profile (10) and increased oxygen metabolism and neovascularization in gliomas (28). Hence, quantitative perfusion parameters may provide vital information for identifying glioma pathologic and molecular characteristics, which can be used as a guide for providing appropriate treatment.

Arterial spin labeling (ASL) perfusion MRI can quantitatively detect cerebral blood flow (CBF) in tissues (15). ASL, which does not require the administration of gadolinium administration, can be an alternative option for patients who are not qualified to undergo contrast-enhanced MRI due to possible renal function impairment caused by gadolinium retention (18). The quantified perfusion status of gliomas on ASL is correlated with histopathologic vascular density (24). Moreover, the distinct blood supply of solid tumor portions has been confirmed in low- and high-grade gliomas (11,24,32). Several studies have emphasized the application of CBF maps in stratifying the genetic risk factors of glioma, such as IDH1/2

genotypes (5,21). Due to the natural diffusive growth pattern of gliomas, quantitative features, such as mean value, are not comprehensive enough in describing the spatial distribution of CBF in gliomas. However, few studies have revealed the correlation between three-dimensional (3D) histogram features on ASL and IDH genetic characteristics. Moreover, the noninvasive quantified CBF value varies with age. The ratio of gray matter-to-white matter perfusion significantly decreased with increasing age (26). Absolute tumor blood flow is less important in glioma grading than the ratio of tumor blood flow-to-age-dependent mean brain perfusion (32). Therefore, age at diagnosis should be included as a concomitant variable in the ASL-related diagnostic test.

This retrospective study aimed to identify the diagnostic efficacy of perfusion histogram features in differentiating IDH genotypes and tumor malignancies. Considering that patients with IDH-mut gliomas are generally younger than those with IDH-wt gliomas (9,13), the accuracy of integrating 3D perfusion histogram features with patient age in identifying glioma genetic features and pathologic characteristics was also validated.

■ MATERIAL and METHODS

The current study was approved by the Institutional Review Board of the institution. Further, it was performed in accordance with the basic principles of the Declaration of Helsinki (The approved data was 12, June, 2019 with the approved number of B2019-085-01).

In total, 131 patients who underwent MRI studies from August 2014 to August 2019 were included in this retrospective study. The need for a written informed consent was waived. The inclusion criteria were as follows: patients with a suspected brain mass and those who underwent routine MRI and ASL. The exclusion criteria were as follows: patients without a pathologically confirmed diagnosis, those with non-glioma lesions, and those without measurable tumor solid portions. There were 91 patients with confirmed gliomas on histologic examinations. Among them, 85 were included in the IDH genotype prediction and 89 in the examination for differentiating glioma grades. Figure 1A shows the study flowchart.

Scanning Protocols

MRI data acquisition was completed using 3.0 T MRI scanner (SIGNA Pioneer or Discovery 750 or Discovery 750W; GE Healthcare, Waukesha, WI, USA) with axial acquisitions. The scanning protocol included the following MRI sequences: T2-weighted fast spin-echo MRI, T1-weighted fluid-attenuated inversion recovery MRI, T2-weighted fluid-attenuated inversion recovery MRI, and contrast-enhanced T1-weighted MRI (T1+C) MRI. The slice thickness was 5 mm with a slice gap of 1 mm, thereby resulting in 22–26 slices covering the entire brain. For ASL, a pseudo-continuous pulse sequence was applied before gadolinium administration. The detailed parameters of ASL were as follows: field of view: 240 x 240 mm²; repetition time: 4597–5241 ms; time to echo: 10.47–10.86 ms; matrix size: 128 × 128; post-label delay time: 1525 ms; slice thickness/slice gap: 4.0/0.0 mm; number of

excitations: 3 (equals to average); and 512 points with 8 arms with a total acquisition time of approximately 4.5 mins.

Volumes of Interest

All anatomic images were co-registered and resampled to T1+C images via SPM (Wellcome Department of Imaging Neuroscience, London, UK; http://www.fil.ion.ucl.ac.uk/spm/software/spm12/). To obtain the tumor volumes of interests (VOIs), a deep learning-based segmentation model implemented in CaPTK (http://www.cbica.upenn.edu/captk) was used to generate VOIs based on all anatomic MRI images with a dual pathway, depth of 11 layers, and 3D convolutional neural network (16). Then, the segmented VOIs were manually corrected by a neuroradiologist with 5 years of experience. The representative regions of interest (ROIs) were displayed by overlaying ROIs on anatomic images, as shown in Figures 2 and 3.

Data Processing and Histogram Feature Extraction

The ASL data were quantified in MATLAB R2013a (www.mathworks.com) according to the general model (6), as implemented in the Functool software of the GE workstation (Advantage Workstation 4.3; GE Medical System, Waukesha, WI, USA). The generated whole-brain CBF maps were then normalized to a standard normal distribution (mean value: 0, standard error: 1) for histogram feature extraction. Ten histogram features describing the distribution of CBF (5th, 10th, 30th, 50th, 70th, 90th, and 95th percentiles and mean) and the dispersion degree of CBF (standard deviation [SD], coefficient of variation [CV]) were then calculated using MATLAB with the in-house software. Figure 1B shows the details of histogram features.

Histological Analysis

Tumor grades were diagnosed using the criteria proposed by the 2021 World Health Organization classification for central nervous system tumors (23). Identifying the IDH genotypes of gliomas was tested via next-generation sequencing or immunohistochemistry. Then, the genotypes were subsequently divided into IDH1-mut and IDH1-wt gliomas.

Statistical Analysis

To explore the correlations between perfusion histogram features as well as tumor grades and IDH genotypes, Spearman's correlation analysis was performed. The differences in histogram features and age at diagnosis between IDH-mut and IDH-wt gliomas were tested using the unpaired t-test. Further, the differences in tumor grade and gender composition in different glioma groups were evaluated using the Fisher's exact test. To combine multiple covariates and to reduce the collinearity of multiple variables, binary logistic regression was used to establish combined models for predicting tumor malignancies and IDH genotypes, which was implemented with the stepwise forward regression method based on maximum likelihood estimation. Receiver operating characteristic curves were utilized to evaluate the diagnostic performance of all included variables and the obtained models. The best cutoff value, sensitivity, and specificity were obtained by as-
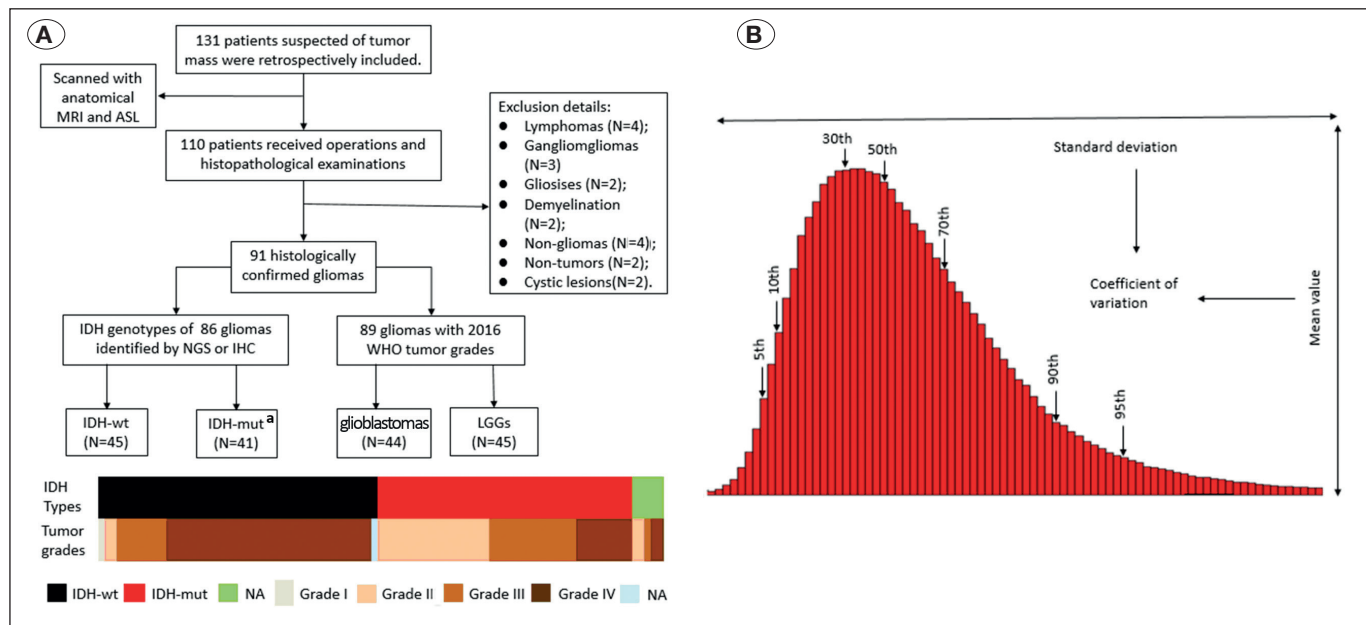

Figure 1: Patient selection flowchart. **Note: ASL:** arterial spin labeling; **NGS:** next-generation sequencing; **IHC:** immunohistochemistry; **IDH:** isocitrate dehydrogenase. The other four tumor types included meningioma, medulloblastoma, gliosarcoma, and metastatic tumor. In the two nontumor included cases, the patients presented with an epidermoid cyst and a post-treatment effect. There were no measurable tumor solids in two cases i.e., one patient had a small tumor, and the other had an excessively bleeding tumor. In IDH genotype prediction, five gliomas without the IDH testing were excluded. While differentiating glioma malignancies, one glioma with an uncertain tumor grade and one pilocytic astrocytoma (grade I) were excluded. The detailed distribution of tumor grades in isocitrate dehydrogenase wild-type and isocitrate dehydrogenase mutant-type gliomas is listed in the color bar map.
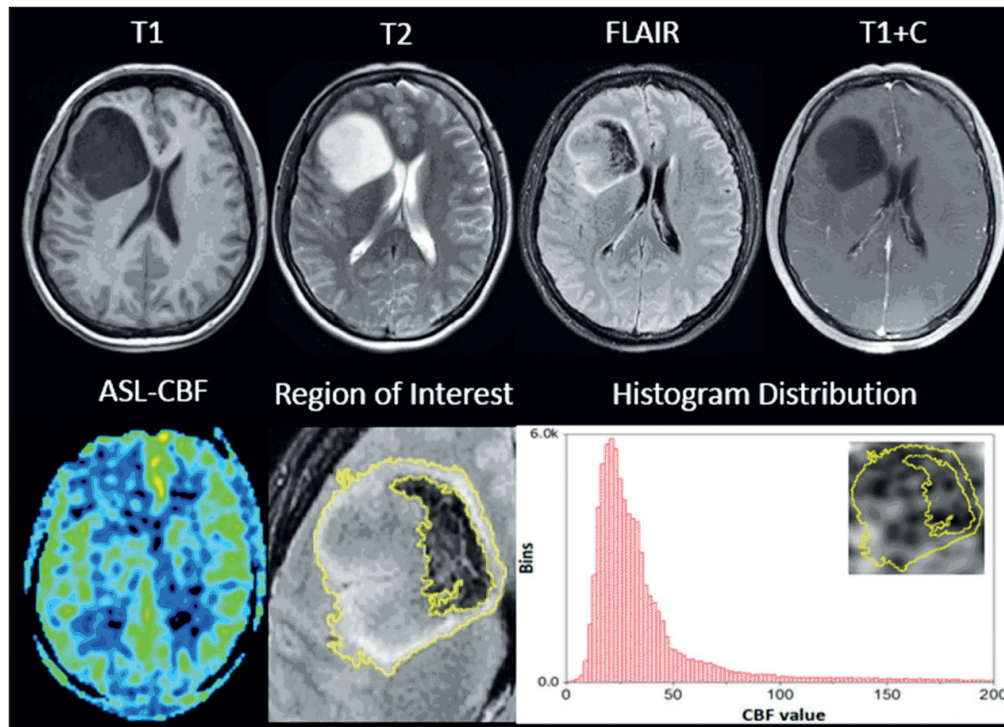
Figure 2: Representative case of isocitrate dehydrogenase mutant and lower-grade gliomas. A 28-year-old woman was diagnosed with diffuse astrocytoma (grade II), The right frontal lesion with long T2 and T1 showed no evident enhancement with a sharply defined boundary. A representative region of interest was overlaid on fluid-attenuated inversion recovery MRI. Compared with the contralateral normal brain, the lesion had a relatively low perfusion with a laterally distributed perfusion histogram.
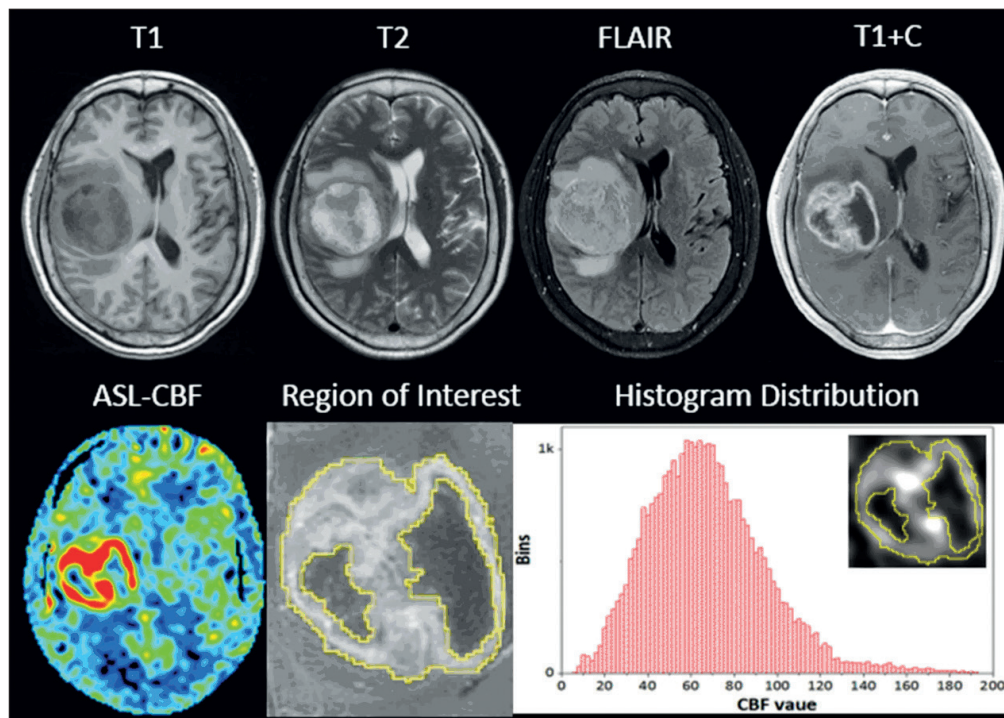
Figure 3: Representative case of isocitrate dehydrogenase wild-type and grade IV gliomas. A 63-year-old woman with glioblastoma (grade IV). The lesion with a heterogeneous signal of iso- or hyper-intensity on T2-weighted imaging was surrounded by edematous tissues. Necrosis was clearly observed with a peripheral ring or patchy enhancement. A representative region of interest was overlaid on contrast-enhanced T1-weighted MRI. Increased perfusion can be observed with a relatively higher central value of the histogram map.

sessing the area under the receiving operating characteristic curve (AUC) based on the maximum Youden index. All statistical analyses were performed using the Statistical Package for the Social Sciences software (version 18.0; IBM, Armonk, NY, USA). A two-tailed p-value of <0.05 was considered statistically significant. For multiple comparison corrections, the Bonferroni-corrected p-value was set at 0.0025 (0.05/20).

◼ RESULTS

Demographic Information and Pathologic Results

There were no significant differences in IDH identification in terms of sex (p=0.204; Table I). However, patients with IDH-mut gliomas were significantly younger than those with IDH-wt gliomas (p<0.0001; Table I). Further, patients with LGGs were significantly younger than those with glioblastomas (42.46 ± 13.19 vs. 49.18 ± 14.41 years, p=0.009). Moreover, the tumor grades according to IDH genotypes significantly differed (p<0.0001; Table I). Patients with LGG were more likely to present with IDH-mt gliomas, and IDH-wt gliomas were often observed in patients with glioblastomas. Figure 1A depicts the detailed composition of tumor grades in different IDH genotypes.

Correlation and Difference Analyses between ASL Histogram Features as Well as Tumor Grades and IDH Genotypes

Figures 2 and 3 show the representative cases on the CBF map and histogram distribution in IDH-mut gliomas/LGGs and IDH-wt gliomas/glioblastoma. Features describing the CBF distribution characters correlated closer than features quantifying CBF dispersion degree. The 5th, 10th, 30th, 50th, and 70th percentiles and mean were significantly correlated with tumor grades (R=0.35–0.36, p<0.0025). The 90th and 95th percentiles, SD, and CV were significantly correlated with tumor grades (p<0.05, and R: 0.31–0.21). The 5th, 10th, 30th, 50th, and 70th percentiles, mean, and CV were significantly correlated with the IDH genotypes (p-value less than the

Bonferroni-corrected p-value: 0.0025 and absolute R: 0.31–0.41). Only the 90th percentile had a p-value of <0.05 (R = 0.26). Further, there were no significant correlations between the 95th percentile and SD as well as the IDH genotypes (R: 0.23–0.19).

Compared with patients with IDH-mut gliomas and LGGs, those with IDH-wt gliomas and glioblastomas had a relatively higher perfusion status. Patients with IDH-wt gliomas and glioblastomas had a significantly greater 5th, 10th, 30th, 50th,
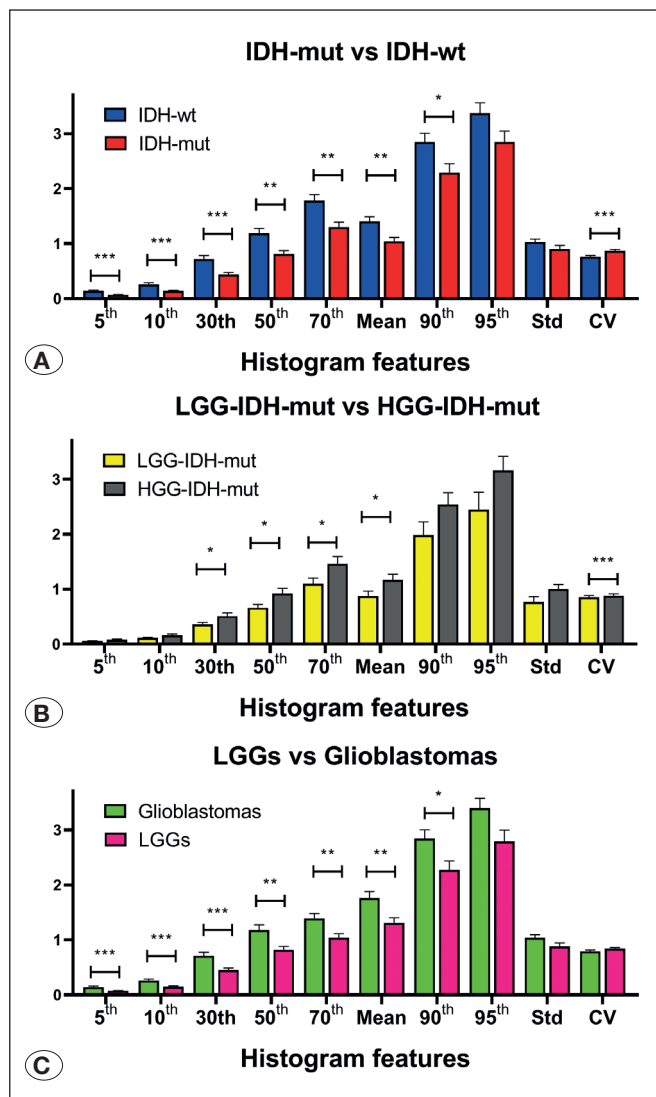
Figure 4: Difference analysis of CBF histogram features in low-grade gliomas versus glioblastomas and isocitrate dehydrogenase wild-type versus isocitrate dehydrogenase mutant-type gliomas. **A)** CBF histogram features in low-grade gliomas versus glioblastomas. **B)** CBF histogram features in isocitrate dehydrogenase mutant-type versus isocitrate dehydrogenase wild-type gliomas. The three asterisks (***) represent a p-value of ≤0.001. The double asterisks (**) represent a p-value of >0.01 and ≤0.001. A single asterisk (*) represents a p-value of ≤0.05, and features without an asterisk represent no significant differences in glioma subtypes. **CBF:** cerebral blood flow.

Table I: Demographical Information and Histological Characteristics

Characters		IDH-wt	IDH-mut	p-value
Gender	F	18	21	0.20
	M	27	20	
Age		52.09 ± 15.10	37.68 ± 9.01	**<0.0001**
Tumor Grades* (n=85)	I	1	0	**<0.0001**
	II	2	18	
	III	8	14	
	IV	33	9	

*The differences of gender composition and tumor grades in IDH-wt and IDH-mut were tested with Fisher's exact test, and the difference of age was tested with independent T-test. *: one patient was excluded for uncertain tumor grade. P-value less than 0.05 is regarded as significant difference.*

70th, and 90th percentiles and mean than those with IDH-mut gliomas and LGGs (Figure 4). Moreover, patients with IDH-wt gliomas had a significantly lower CV than those with IDH-mut gliomas, and there were no significant differences in terms of the 95th percentile and SD (Figure 4). Glioblastomas had a significantly higher 95th percentile than LGGs. However, the SD and CV did not significantly differ between glioblastomas and LGGs (Figure 4).

Diagnostic Performances of ASL Histogram Features in Differentiating IDH Genotypes From Glioma

The AUCs of histogram features in differentiating LGGs from glioblastomas varied from 0.61 to 0.67, and the features commonly had an AUC of 0.67 (Table II). Generally, the AUCs of histogram features derived from perfusion parameters in differentiating IDH-mut from IDH-wt gliomas were approximately 0.7. The 5th percentile had the best diagnostic performance in differentiating IDH-wt from IDH-mut gliomas, with an AUC of 0.744 (sensitivity: 70.5%, specificity: 73.2%). Table II shows the detailed AUCs, sensitivity, and specificity for diagnostic assessments.

Combined Perfusion Histogram Features and Non-Radiographic Information in Differentiating Glioma Subtypes

In differentiating LGGs from glioblastomas, the AUC, sensitivity, and specificity of age at diagnosis were 0.672%, 47.7%, and 87.0%, respectively. The combined application of ASL histogram features and age at diagnosis had a better AUC at 0.73, with a sensitivity and specificity of 70.5% and 71.1%, respectively (Figure 5). The combined model can be expressed as follows: the probability of glioblastoma = 2.078 × CBF 30th percentile + 0.037 × age - 2.89. In differentiating IDH-mut from IDH-wt gliomas, age at diagnosis exhibited diagnostic performances with an AUC of 0.782, sensitivity of 63.6%, and specificity of 87.8%. The combined model including age at diagnosis and CBF 10th percentile can be expressed as follows: Y (the probability of IDH type) = −7.605 × CBF 10th percentile −0.093 × age + 5.538. The combined model could be more effective in differentiating IDH-wt and IDH-mut gliomas with an AUC of 0.86 and an improved sensitivity and specificity of 84.4% and 82.9%, respectively (Figure 5).

■ DISCUSSION

This retrospective study aimed to evaluate significant correlations between noninvasive perfusion histogram features and IDH genotypes as well as tumor grades. CBF histogram features revealed the distinct distribution of the tumor blood supply among glioma subtypes. Furthermore, they can effectively differentiate IDH-mut from IDH-wt gliomas, and LGGs from glioblastomas. The models using both age at diagnosis and CBF histogram features have a higher accuracy in identifying glioma IDH genotypes and tumor malignancies.

Our results also showed that perfusion-weighted histogram features extracted from three-dimensional VOIs were significantly correlated with glioma IDH genotypes and glioma malignancies. Moreover, they can efficiently distinguish different glioma subtypes. Genetic types and pathologic grades have a great impact on glioma vascularization. From a genetic aspect, IDH-mut gliomas have significantly low neovascularization (19). In contrast, IDH-wt gliomas have a specific angiogenic gene expression signature (39). Inhibitors targeting the IDH pathway have reduced angiogenesis and contribute to vascular normalization (12). With increasing tumor grade, tumor cell proliferation is more rapid and requires more blood supply accompanying microcirculatory changes during tumor

Table II: The Diagnostic Performances of Histogram Features In Differentiating LGGs vs Glioblastomas, and IDH-mut vs IDH-wt

Features	IDH-mut vs IDH-wt			LGGs vs Glioblastomas		
	AUC	Sen. (%)	Spec. (%)	AUC	Sen. (%)	Spec. (%)
5th	0.74	70.5	73.2	0.67	56.8	73.34
10th	0.74	70.5	73.2	0.67	54.5	75.6
30th	0.71	52.3	82.9	0.67	50.0	82.2
50th	0.70	59.1	75.6	0.67	31.8	97.8
Mean	0.69	68.2	63.4	0.67	65.9	64.4
70th	0.69	68.2	65.9	0.67	65.9	60.0
90th	0.65	77.3	51.2	0.64	81.8	46.7
95th	0.63	73.3	53.6	0.65	88.6	46.7
Std	0.61	84.4	43.9	0.64	88.6	48.9
CV	0.69	82.9	55.6	0.61	82.2	47.7
Combined model	0.86	84.4	82.9	0.73	70.5	71.1

AUC: Area under the curve, CI: Confidence interval, Sen.: Sensitivity, Spec.: Specificity, CV: Coefficient of variation, IDH-mut: Isocitrate dehydrogenase mutant-type, IDH-wt: Isocitrate dehydrogenase wild-type, LGGs: Low grade gliomas.
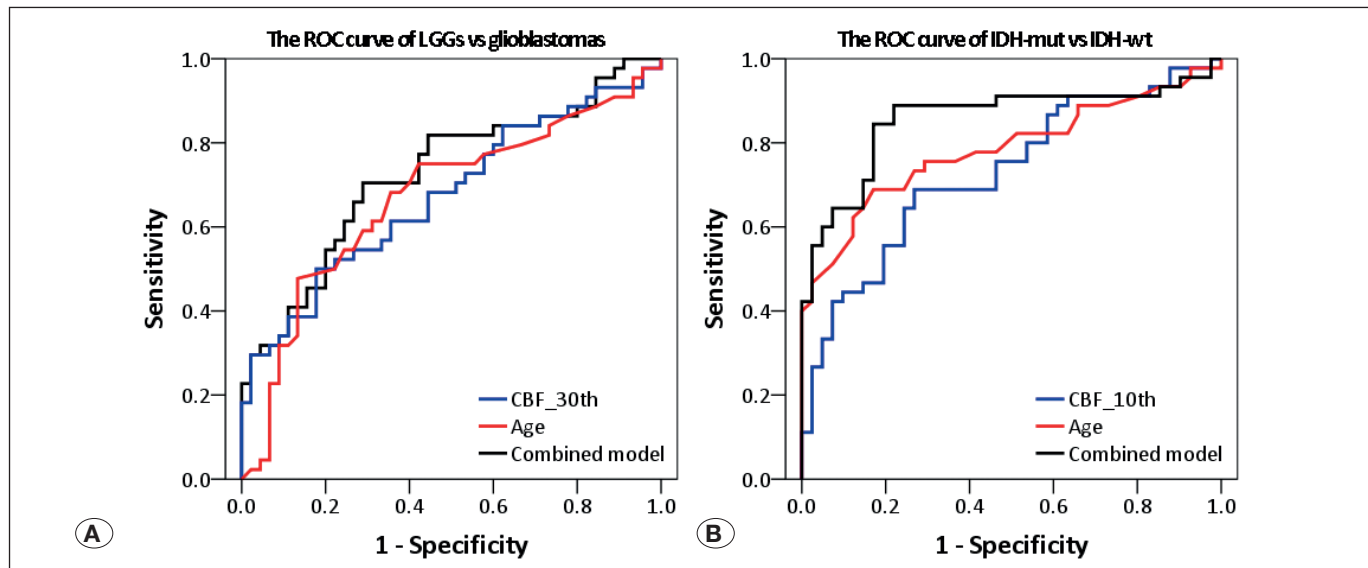
Figure 5: Receiver operating characteristic curve of combined models for differentiating lower-grade gliomas from glioblastomas and isocitrate dehydrogenase mutant-type from isocitrate dehydrogenase wild-type gliomas. The combined model of CBF 30th percentiles and age at diagnosis improved the area under the curve to 0.73 in differentiating low-grade gliomas and glioblastomas with the following equation: the probability of glioblastoma = $2.078 \times$ CBF_30th percentile + $0.037 \times$ age - 2.89. The combined model included age at diagnosis and perfusion histogram features (CBF_10th percentile) with the following expression: the probability of isocitrate dehydrogenase type = $-7.605 \times$ CBF_10th percentile $- 0.093 \times$ age + 5.538. Evident improvement in differentiating isocitrate dehydrogenase genotypes was achieved, with an area under the curve of 0.86. **CBF:** cerebral blood flow.

growth (8,29). Hence, evaluating glioma subtypes with non-invasive perfusion-weighted MRI could yield profound outcomes, which are consistent with our results.

ASL can be used for the noninvasive quantification of *in vivo* tissue perfusion without the need for gadolinium administration and can serve as a state-of-the-art cerebral angiographic measurement technique for research and clinical studies (15). As detected using ASL in our study, malignant gliomas with highly invasive behaviors commonly manifest with high perfusion status, which is in accordance with a previous study (38). Several studies have focused on the application of ASL in grading gliomas (36). Nevertheless, no related research has reported its usage in differentiating LGGs from glioblastomas, which was emphasized in our study. Several studies have investigated the application of ASL in differentiating glioma gene signatures (5,21,37). Our study showed the high perfusion status of solid tumor portions within IDH-wt gliomas, and this result was in accordance with that of previous reports (5,21,37). With a relatively larger data sample of patients with glioma (27), our results might be more persuasive. With 3D histogram analysis, the interspace distributions of ASL can be more accurately described by histogram features than mean values from a single slice (5), thereby allowing a more comprehensive comparison of perfusion status in IDH-wt and IDH-mut gliomas.

The combined predictive models obtained in our study have used patient age and achieved better AUCs in predicting higher invasive glioma types. Further, age at diagnosis was significantly correlated with IDH genetic phenotypes and tumor grades in our study, which is also similar to that of previous

studies (4,9). Compared with younger patients, older patients commonly present with IDH-wt gliomas, and they have a poor survival (9). Elderly patients frequently develop IDH-wt gliomas and glioblastomas (9,13,35). However, previous studies have identified age-associated reductions in CBF (7,26), which indicates that age can be a confounding factor in identifying tumor perfusion status. The integration of patient age with radiographic features is important for noninvasive prediction toward higher stratification factors (32). With the implementation of logistic regression analysis to overcome the multicollinearity of variables, predictive models using combined age at diagnosis and ASL histogram features have been established with a better identification accuracy in our study. The appropriate treatment strategies for gliomas include radio- and chemo-sensitivity options, and radiation dosage planning is based on an accurate diagnosis of histopathologic grades and genetic molecular features (30). Considering the effect of IDH genotypes on lymphocyte infiltration and PD-L1 expression status (3) and possible effects on the development of treatment strategies (17), the model with combined features for predicting IDH genotypes might provide vital information for glioma immunotherapy.

The current study had several limitations. First, although ASL images have been co-registered to anatomic MRI, the mismatched thickness of perfusion and T1+C MRI might cause potential bias due to interpolation. Second, 3D ASL histogram features were calculated from whole solid tumor parts. Meanwhile, the pathologic examination of genetic characteristics and tumor grades was performed using stained tissue specimens. The mismatch between MRI measurement and tissue

samples might introduce potential selection bias. Third, the stratification of glioma risk factors (grades and IDH types) was based on the VOIs identified on T1+C post-contrast images. ASL does not require the administration of gadolinium. Thus, similar results could have been obtained using ASL features from tumor regions outlined by noncontrast-enhanced MRI, rather than T1+C MRI.

■ CONCLUSION

Noninvasive ASL histogram features were significantly correlated with glioma IDH genotypes and tumor malignancies, and they could effectively differentiate various glioma subtypes. Both age at diagnosis and perfusion-weighted histogram features could effectively differentiate IDH-wt from IDH-mut gliomas. However, the combined models could facilitate a more comprehensive evaluation of glioma invasiveness and lead to a higher identification accuracy. Hence, ASL is a useful noninvasive assessment tool for gliomas before surgical intervention.

■ ACKNOWLEDGEMENT

AUTHORSHIP CONTRIBUTION

Study conception and design: CS, RJ, CP

Data collection: CP, CS

Analysis and interpretation of results: YS, RJ, FCD

Draft manuscript preparation: CS, RJ

Critical revision of the article: CX, KC, FCD

Other (study supervision, fundings, materials, etc...): CS, CX

All authors (CS, CP, YS, FCD, RJ, CX, KC) reviewed the results and approved the final version of the manuscript.

■ REFERENCES

1. Agnihotri S, Aldape KD, Zadeh G: Isocitrate dehydrogenase status and molecular subclasses of glioma and glioblastoma. Neurosurg Focus 37:E13, 2014. https://doi.org/10.3171/2014.9.FOCUS14505

2. Aoki K, Nakamura H, Suzuki H, Matsuo K, Kataoka K, Shimamura T, Motomura K, Ohka F, Shiina S, Yamamoto T, Nagata Y, Yoshizato T, Mizoguchi M, Abe T, Momii Y, Muragaki Y, Watanabe R, Ito I, Sanada M, Yajima H, Morita N, Takeuchi I, Miyano S, Wakabayashi T, Ogawa S, Natsume A: Prognostic relevance of genetic alterations in diffuse lower-grade gliomas. Neuro-oncology 20:66-77, 2018. https://doi.org/10.1093/neuonc/nox132

3. Berghoff AS, Kiesel B, Widhalm G, Wilhelm D, Rajky O, Kurscheid S, Kresl P, Wohrer A, Marosi C, Hegi ME, Preusser M: Correlation of immune phenotype with IDH mutation in diffuse glioma. Neuro Oncol 19:1460-1468, 2017. https://doi.org/10.1093/neuonc/nox054

4. Brat DJ, Verhaak RG, Aldape KD, Yung WK, Salama SR, Cooper LA, Rheinbay E, Miller CR, Vitucci M, Morozova O, Robertson AG, Noushmehr H, Laird PW, Cherniack AD, Akbani R, Huse JT, Ciriello G, Poisson LM, Barnholtz-Sloan JS, Berger MS, Brennan C, Colen RR, Colman H, Flanders AE, Giannini C, Grifford M, Iavarone A, Jain R, Joseph I, Kim J, Kasaian K, Mikkelsen T, Murray BA, O'Neill BP, Pachter L, Parsons DW, Sougnez C, Sulman EP, Vandenberg SR, Van Meir EG, von Deimling A, Zhang H, Crain D, Lau K, Mallery D, Morris S, Paulauskis J, Penny R, Shelton T, Sherman M, Yena P, Black A, Bowen J, Dicostanzo K, Gastier-Foster J, Leraas KM, Lichtenberg TM, Pierson CR, Ramirez NC, Taylor C, Weaver S, Wise L, Zmuda E, Davidsen T, Demchok JA, Eley G, Ferguson ML, Hutter CM, Mills Shaw KR, Ozenberger BA, Sheth M, Sofia HJ, Tarnuzzer R, Wang Z, Yang L, Zenklusen JC, Ayala B, Baboud J, Chudamani S, Jensen MA, Liu J, Pihl T, Raman R, Wan Y, Wu Y, Ally A, Auman JT, Balasundaram M, Balu S, Baylin SB, Beroukhim R, Bootwalla MS, Bowlby R, Bristow CA, Brooks D, Butterfield Y, Carlsen R, Carter S, Chin L, Chu A, Chuah E, Cibulskis K, Clarke A, Coetzee SG, Dhalla N, Fennell T, Fisher S, Gabriel S, Getz G, Gibbs R, Guin R, Hadjipanayis A, Hayes DN, Hinoue T, Hoadley K, Holt RA, Hoyle AP, Jefferys SR, Jones S, Jones CD, Kucherlapati R, Lai PH, Lander E, Lee S, Lichtenstein L, Ma Y, Maglinte DT, Mahadeshwar HS, Marra MA, Mayo M, Meng S, Meyerson ML, Mieczkowski PA, Moore RA, Mose LE, Mungall AJ, Pantazi A, Parfenov M, Park PJ, Parker JS, Perou CM, Protopopov A, Ren X, Roach J, Sabedot TS, Schein J, Schumacher SE, Seidman JG, Seth S, Shen H, Simons JV, Sipahimalani P, Soloway MG, Song X, Sun H, Tabak B, Tam A, Tan D, Tang J, Thiessen N, Triche T, Jr., Van Den Berg DJ, Veluvolu U, Waring S, Weisenberger DJ, Wilkerson MD, Wong T, Wu J, Xi L, Xu AW, Zack TI, Zhang J, Aksoy BA, Arachchi H, Benz C, Bernard B, Carlin D, Cho J, DiCara D, Frazer S, Fuller GN, Gao J, Gehlenborg N, Haussler D, Heiman DI, Iype L, Jacobsen A, Ju Z, Katzman S, Kim H, Knijnenburg T, Kreisberg RB, Lawrence MS, Lee W, Leinonen K, Lin P, Ling S, Liu W, Liu Y, Lu Y, Mills G, Ng S, Noble MS, Paull E, Rao A, Reynolds S, Saksena G, Sanborn Z, Sander C, Schultz N, Senbabaoglu Y, Shen R, Shmulevich I, Sinha R, Stuart J, Sumer SO, Sun Y, Tasman N, Taylor BS, Voet D, Weinhold N, Weinstein JN, Yang D, Yoshihara K, Zheng S, Zhang W, Zou L, Abel T, Sadeghi S, Cohen ML, Eschbacher J, Hattab EM, Raghunathan A, Schniederjan MJ, Aziz D, Barnett G, Barrett W, Bigner DD, Boice L, Brewer C, Calatozzolo C, Campos B, Carlotti CG, Jr., Chan TA, Cuppini L, Curley E, Cuzzubbo S, Devine K, DiMeco F, Duell R, Elder JB, Fehrenbach A, Finocchiaro G, Friedman W, Fulop J, Gardner J, Hermes B, Herold-Mende C, Jungk C, Kendler A, Lehman NL, Lipp E, Liu O, Mandt R, McGraw M, McLendon R, McPherson C, Neder L, Nguyen P, Noss A, Nunziata R, Ostrom QT, Palmer C, Perin A, Pollo B, Potapov A, Potapova O, Rathmell WK, Rotin D, Scarpace L, Schilero C, Senecal K, Shimmel K, Shurkhay V, Sifri S, Singh R, Sloan AE, Smolenski K, Staugaitis SM, Steele R, Thorne L, Tirapelli DP, Unterberg A, Vallurupalli M, Wang Y, Warnick R, Williams F, Wolinsky Y, Bell S, Rosenberg M, Stewart C, Huang F, Grimsby JL, Radenbaugh AJ: Comprehensive, integrative genomic analysis of diffuse lower-grade gliomas. N Engl J Med 372: 2481-2498, 2015

5. Brendle C, Hempel JM, Schittenhelm J, Skardelly M, Tabatabai G, Bender B, Ernemann U, Klose U: Glioma grading and determination of IDH mutation status and ATRX loss by DCE and ASL perfusion. Clin Neuroradiol 28:421-428, 2018. https://doi.org/10.1007/s00062-017-0590-z

6. Buxton RB, Frank LR, Wong EC, Siewert B, Warach S, Edelman RR: A general kinetic model for quantitative perfusion imaging with arterial spin labeling. Magn Reson Med 40:383-396, 1998. https://doi.org/10.1002/mrm.1910400308

7. Chen JJ, Rosas HD, Salat DH: Age-associated reductions in cerebral blood flow are independent from regional atrophy. Neuroimage 55:468-478, 2011. https://doi.org/10.1016/j.neuroimage.2010.12.032

8. Chen WJ, He DS, Tang RX, Ren FH, Chen G: Ki-67 is a valuable prognostic factor in gliomas: Evidence from a systematic review and meta-analysis. Asian Pac J Cancer Prev 16:411-420, 2015. https://doi.org/10.7314/APJCP.2015.16.2.411

9. Eckel-Passow JE, Lachance DH, Molinaro AM, Walsh KM, Decker PA, Sicotte H, Pekmezci M, Rice T, Kosel ML, Smirnov IV, Sarkar G, Caron AA, Kollmeyer TM, Praska CE, Chada AR, Halder C, Hansen HM, McCoy LS, Bracci PM, Marshall R, Zheng S, Reis GF, Pico AR, O'Neill BP, Buckner JC, Giannini C, Huse JT, Perry A, Tihan T, Berger MS, Chang SM, Prados MD, Wiemels J, Wiencke JK, Wrensch MR, Jenkins RB: Glioma groups based on 1p/19q, IDH, and TERT promoter mutations in tumors. N Engl J Med 372: 2499-2508, 2015. https://doi.org/10.1056/NEJMoa1407279

10. Esmaeili M, Hamans BC, Navis AC, van Horssen R, Bathen TF, Gribbestad IS, Leenders WP, Heerschap A: IDH1 R132H mutation generates a distinct phospholipid metabolite profile in glioma. Cancer Res 74:4898-4907, 2014. https://doi.org/10.1158/0008-5472.CAN-14-0008

11. Falk Delgado A, De Luca F, van Westen D, Falk Delgado A: Arterial spin labeling MR imaging for differentiation between high- and low-grade glioma-a meta-analysis. Neuro Oncol 20: 1450-1461, 2018. https://doi.org/10.1093/neuonc/noy095

12. Gargini R, Segura-Collar B, Herranz B, Garcia-Escudero V, Romero-Bravo A, Nunez FJ, Garcia-Perez D, Gutierrez-Guaman J, Ayuso-Sacido A, Seoane J, Perez-Nunez A, Sepulveda-Sanchez JM, Hernandez-Lain A, Castro MG, Garcia-Escudero R, Avila J, Sanchez-Gomez P: The IDH-TAU-EGFR triad defines the neovascular landscape of diffuse gliomas. Sci Transl Med 12:eaax1501, 2020. https://doi.org/10.1126/scitranslmed.aax1501

13. Hartmann C, Meyer J, Balss J, Capper D, Mueller W, Christians A, Felsberg J, Wolter M, Mawrin C, Wick W, Weller M, Herold-Mende C, Unterberg A, Jeuken JW, Wesseling P, Reifenberger G, von Deimling A: Type and frequency of IDH1 and IDH2 mutations are related to astrocytic and oligodendroglial differentiation and age: A study of 1,010 diffuse gliomas. Acta Neuropathol 118:469-474, 2009. https://doi.org/10.1007/s00401-009-0561-9

14. Jason B, Dima S, Hess KR, Fox BD, Vincent C, Matthew C, Nicole S, Gilbert MR, Raymond S, Prabhu SS: IDH1 mutant malignant astrocytomas are more amenable to surgical resection and have a survival benefit associated with maximal surgical resection. Neuro Oncol 16:81-91, 2014. https://doi.org/10.1093/neuonc/not159

15. Jezzard P, Chappell MA, Okell TW: Arterial spin labeling for the measurement of cerebral perfusion and angiography. J Cereb Blood Flow Metab 38:603-626, 2018. https://doi.org/10.1177/0271678X17743240

16. Kamnitsas K, Ledig C, Newcombe VFJ, Simpson JP, Kane AD, Menon DK, Rueckert D, Glocker B: Efficient multi-scale 3D CNN with fully connected CRF for accurate brain lesion segmentation. Med Image Anal 36:61-78, 2017. https://doi.org/10.1016/j.media.2016.10.004

17. Karpel-Massler G, Nguyen TTT, Shang E, Siegelin MD: Novel IDH1-targeted glioma therapies. CNS Drugs 33:1155-1166, 2019. https://doi.org/10.1007/s40263-019-00684-6

18. Kartamihardja AA, Nakajima T, Kameo S, Koyama H, Tsushima Y: Impact of impaired renal function on gadolinium retention after administration of gadolinium-based contrast agents in a mouse model. Invest Radiol 51:655-660, 2016. https://doi.org/10.1097/RLI.0000000000000295

19. Kickingereder P, Sahm F, Radbruch A, Wick W, Heiland S, Deimling A, Bendszus M, Wiestler B: IDH mutation status is associated with a distinct hypoxia/angiogenesis transcriptome signature which is non-invasively predictable with rCBV imaging in human glioma. Sci Rep 5:16238, 2015. https://doi.org/10.1038/srep16238

20. Lee S, Jang Y, Park M, Kim J, Park C: Idh-1 mutation determines health-related quality of life and cognitive deficit after surgery in high grade glioma. Neuro Oncol 19:121, 2017. https://doi.org/10.1093/neuonc/nox036.468

21. Liu T, Cheng G, Kang X, Xi Y, Zhu Y, Wang K, Sun C, Ye J, Li P, Yin H: Noninvasively evaluating the grading and IDH1 mutation status of diffuse gliomas by three-dimensional pseudo-continuous arterial spin labeling and diffusion-weighted imaging. Neuroradiol 60:693-702, 2018. https://doi.org/10.1007/s00234-018-2021-5

22. Louis DN, Perry A, Reifenberger G, von Deimling A, Figarella-Branger D, Cavenee WK, Ohgaki H, Wiestler OD, Kleihues P, Ellison DW: The 2016 World Health Organization Classification of tumors of the central nervous system: A summary. Acta Neuropathol 131:803-820, 2016. https://doi.org/10.1007/s00401-016-1545-1

23. Louis DN, Perry A, Wesseling P, Brat DJ, Cree IA, Figarella-Branger D, Hawkins C, Ng HK, Pfister SM, Reifenberger G, Soffietti R, von Deimling A, Ellison DW: The 2021 WHO Classification of Tumors of the central nervous system: A summary. Neuro Oncol 23:1231-1251, 2021. https://doi.org/10.1093/neuonc/noab106

24. Noguchi T, Yoshiura T, Hiwatashi A, Togao O, Yamashita K, Nagao E, Shono T, Mizoguchi M, Nagata S, Sasaki T, Suzuki SO, Iwaki T, Kobayashi K, Mihara F, Honda H: Perfusion imaging of brain tumors using arterial spin-labeling: Correlation with histopathologic vascular density. AJNR Am J Neuroradiol 29:688-693, 2008. https://doi.org/10.3174/ajnr.A0903

25. Ostrom QT, Bauchet L, Davis FG, Deltour I, Fisher JL, Langer CE, Pekmezci M, Schwartzbaum JA, Turner MC, Walsh KM, Wrensch MR, Barnholtz-Sloan JS: The epidemiology of glioma in adults: A "state of the science" review. Neuro Oncol 16:896-913, 2014. https://doi.org/10.1093/neuonc/nou087

26. Parkes LM, Rashid W, Chard DT, Tofts PS: Normal cerebral perfusion measurements using arterial spin labeling: Reproducibility, stability, and age and gender effects. Magn Reson Med 51:736-743, 2004. https://doi.org/10.1002/mrm.20023

27. Sica GT: Bias in research studies. Radiology 238:780-789, 2006. https://doi.org/10.1148/radiol.2383041109

28. Stadlbauer A, Zimmermann M, Kitzwogerer M, Oberndorfer S, Rossler K, Dorfler A, Buchfelder M, Heinz G: MR Imaging-derived oxygen metabolism and neovascularization characterization for grading and IDH gene mutation detection of gliomas. Radiology 283:799-809, 2017. https://doi.org/10.1148/radiol.2016161422

29. Vajkoczy P, Schilling L, Ullrich A, Schmiedek P, Menger MD: Characterization of angiogenesis and microcirculation of high-grade glioma: An intravital multifluorescence microscopic approach in the athymic nude mouse. J Cereb Blood Flow Metab 18:510-520, 1998. https://doi.org/10.1097/00004647-199805000-00006

30. van den Bent MJ: Interobserver variation of the histopathological diagnosis in clinical trials on glioma: A clinician's perspective. Acta Neuropathol 120:297-304, 2010. https://doi.org/10.1007/s00401-010-0725-7

31. Waitkus MS, Diplas BH, Yan H: Isocitrate dehydrogenase mutations in gliomas. Neuro Oncol 18:16-26, 2016. https://doi.org/10.1093/neuonc/nov136

32. Warmuth C, Gunther M, Zimmer C: Quantification of blood flow in brain tumors: Comparison of arterial spin labeling and dynamic susceptibility-weighted contrast-enhanced MR imaging. Radiology 228:523-532, 2003. https://doi.org/10.1148/radiol.2282020409

33. Weller M, van den Bent M, Tonn JC, Stupp R, Preusser M, Cohen-Jonathan-Moyal E, Henriksson R, Le Rhun E, Balana C, Chinot O, Bendszus M, Reijneveld JC, Dhermain F, French P, Marosi C, Watts C, Oberg I, Pilkington G, Baumert BG, Taphoorn MJB, Hegi M, Westphal M, Reifenberger G, Soffietti R, Wick W: European Association for Neuro-Oncology (EANO) guideline on the diagnosis and treatment of adult astrocytic and oligodendroglial gliomas. Lancet Oncol 18:e315-e329, 2017. https://doi.org/10.1016/S1470-2045(17)30194-8

34. Weller M, Wick W, Aldape K, Brada M, Berger M, Pfister SM, Nishikawa R, Rosenthal M, Wen PY, Stupp R, Reifenberger G: Glioma. Nat Rev Dis Primers 1:15017, 2015. https://doi.org/10.1038/nrdp.2015.17

35. Wen PY, Kesari S: Malignant gliomas in adults. N Engl J Med 359:492-507, 2008. https://doi.org/10.1056/NEJMra0708126

36. Yang S, Zhao B, Wang G, Xiang J, Xu S, Liu Y, Zhao P, Pfeuffer J, Qian T: Improving the grading accuracy of astrocytic neoplasms noninvasively by combining timing information with cerebral blood flow: A multi-ti arterial spin-labeling mr imaging study. AJNR Am J Neuroradiol 37:2209-2216, 2016. https://doi.org/10.3174/ajnr.A4907

37. Yoo RE, Yun TJ, Hwang I, Hong EK, Kang KM, Choi SH, Park CK, Won JK, Kim JH, Sohn CH: Arterial spin labeling perfusion-weighted imaging aids in prediction of molecular biomarkers and survival in glioblastomas. Eur Radiol 30:1202-1211, 2020. https://doi.org/10.1007/s00330-019-06379-2

38. Zeng Q, Jiang B, Shi F, Ling C, Dong F, Zhang J: 3D pseudocontinuous arterial spin-labeling MR imaging in the preoperative evaluation of gliomas. AJNR Am J Neuroradiol 38:1876-1883, 2017. https://doi.org/10.3174/ajnr.A5299

39. Zhang L, He L, Lugano R, Roodakker K, Bergqvist M, Smits A, Dimberg A: IDH mutation status is associated with distinct vascular gene expression signatures in lower-grade gliomas. Neuro Oncol 20:1505-1516, 2018. https://doi.org/10.1093/neuonc/noy088